P6M.2

Using surface pressure variations to study atmospheric disturbances generated by diurnal heating

Yanping Li and Ronald B. Smith
Department of Geology and Geophysics
Yale University, Connecticut, USA

1. Phenomena:

Solar heating generates a diurnal cycle in temperature, winds and pressure over the Earth. The direct solar heating of the atmosphere (e.g. absorption by ozone in the stratosphere) can act everywhere (Chapman and Lindzen, 1970), whereas indirect heating through surface fluxes will be inhomogeneous. Over land, the surface receives heat and transports it upward by small scale convection. The Rocky Mountains is a typical area for this (Banta and Schaaf, 1987). Several responses to diurnal heating are possible, e.g. sea breeze and mountain–plain circulation. Carbone et al. (2002), using radar composites, found eastward propagating diurnal precipitation systems over the Great Plains and the Mid-west, moving at a speed of about 20m/s.

In some other areas, such as the Bay of Bengal, satellites reveal a diurnal disturbance spreading southeastward parallel to the coast in winter with a propagation speed between 15 and 20 m/s (Yang and Slingo, 2001). In South America, diurnal convection propagates from the Andean ridge westward over the sea at a speed about 12m/s (Mapes et al, 2003).

The goal of this paper is to use hourly pressure data to reveal more properties of diurnal circulations.

2. Data analysis methods:

The daily observed meteorological data like station pressure or sea level pressure data is a well recorded hourly data at hundreds of ASOS (Automated Surface Observing System) sites in the USA. By doing a harmonic analysis, we obtained the diurnal component of the surface pressure with their amplitude and phase distribution over the United States (Mass et al, 1991). Our calculated phase of the diurnal component is given by the local solar time when the diurnal component of the surface pressure disturbance reaches its maximum. Local solar time is 12AM at the moment that the sun crosses the local meridian. It can also be calculated by doing a longitude correction to the local standard time or UTC there.

Harmonic analysis:

$$\mathrm{Re}_n = \sum_{k=1}^{N} P_n(k)\cos\frac{2\pi k\times 24}{N} \qquad \mathrm{Im}_n = \sum_{k=1}^{N} P_n(k)\sin\frac{2\pi k\times 24}{N}$$

$$C_n = \sqrt{\mathrm{Re}_n{}^2 + \mathrm{Im}_n{}^2} \qquad \psi_n = a\tan\left(\frac{\mathrm{Im}_n}{\mathrm{Re}_n}\right)\times\frac{360}{2\pi}$$

The phase correction between local solar time and local standard time for station n:

$$\psi_n' = \psi_n + TimeZone(n)\times 15^{\circ} + longitude(n)$$

Here, ψ_n is the calculated phase angle relative to the local standard time; ψ_n' is the phase angle related to the local solar time. For example, $\psi_n' = 0^{\circ}$ implies pressure maximum at 0000 local solar time whereas $\psi_n' = 105^{\circ}$ implies 0700 local solar time for pressure maximum and 1900 for minimum.

Our interpretation of the data is guided by the assumption that the diurnal signal is the sum of three parts

- Global atmospheric tide driven mostly by solar heating of the stratosphere (westward moving at about 350m/s at $40^{\circ}N$).
- Continentally enhanced Tide driven by surface heat fluxes.
- Mesoscale disturbance related to variations in the earth surface (mountain, coast, or land cover). These disturbances are driven locally by surface heat flux gradients, but they can propagate away using various mechanisms: e.g. gravity waves, PV pulses, storm dynamics.

We call the sum of the first and the second parts as the atmospheric tide, since it has the same west-propagating speed as that of the Sun. This atmospheric tide may vary for different regions. If we know the atmospheric tide, we can obtain the local diurnal mesoscale disturbance by a simple vector subtraction. Our assumption is:

Diurnal component of the observed surface pressure $C_n e^{i(\omega t+\psi_n)}$

= Diurnal atmospheric tide $Ae^{i(\omega t+\theta)}$

+Local thermally generated mesoscale signal $B_n e^{i(\omega t+\varphi_n)}$

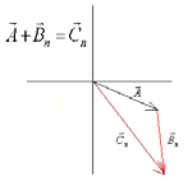

Figure 1: Vector diagram showing the additive property of the diurnal components of the surface pressure for station n. $\vec{A}$ is the diurnal atmospheric tide. $\vec{B}$ is the local thermally generated mesoscale disturbance. $\vec{C}$ is the total diurnal component of the observed surface pressure.

3. Linear model simulations:

In order to study the local mesoscale part of diurnal surface pressure variation, we use an analytical-FFT model based on the linearized Boussinesq equations.

Simulations 1 and 2 are based on vertically exponential diurnal heating, medium Coriolis effect, no vertical shear, without mean wind/with easterly wind. The generated surface pressure disturbances are shown in Figure 2 and 3 in amplitude and phase. It seems that the diurnal heating generated inertio-gravity waves (IGW). Local surface pressure disturbance has amplitude maximum and phase minimum at the heating source. Without mean wind, the two centers are the same. In Figure 2, the disturbance at the center has amplitude 40Pa and phase 30°. About 50km away from the center, the disturbance decreases to 20Pa and phase becomes 35°(i.e. 20 minutes delay). Compared Figure 2 and 3,

it can be seen that the effect of the mean wind is to shift the two centers in opposite directions: The amplitude isolines shift downwind and the phase isolines shift upwind.

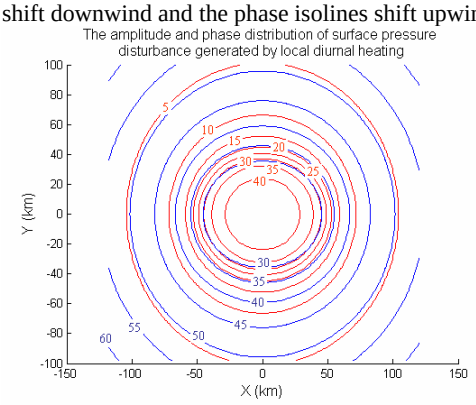

Figure 2: Simulation 1. Amplitude (red) and phase (blue) of the surface pressure disturbance generated by the local diurnal heating with $f = 6.8\times10^{-5}$, $H = 1000m$ $U = V = 0m/s$.

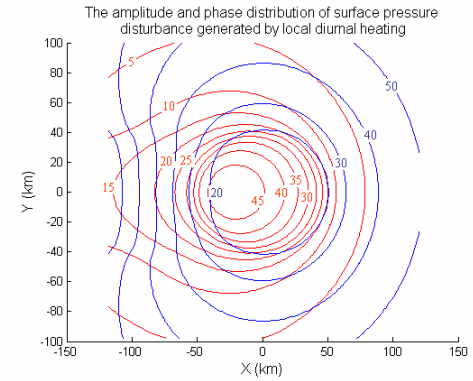

Figure 3: Simulation 2. Like figure 2 but with $U = -5m/s$.

Simulations 3 and 4 are based on elevated diurnal heating, strong vertical mean wind shear, with weak/strong Coriolis effect. The generated potential vorticity (PV) in the upper level (z=5200m), the pressure disturbance at the surface, the vertical velocity perturbation w' in the lower level (z=1900m) and the phase distribution of the surface pressure disturbance are shown in Figure 4 and 5 in a time-distance plot for each simulation.

Figure 4 shows simulation 3 with weak Coriolis effect ($f = 10^{-5}s^{-1}$). From the slopes of these time-distance plots we can see that the upper PV is advecting with the upper steering wind, but the surface pressure disturbance and w' are propagating together at a slower speed. IGWs dominate due to the weak Coriolis effect.

Figure 5 shows simulation 4 with strong Coriolis effect ($f = 10^{-4}s^{-1}$). The slopes of these time-distance plots show that near the heating source, the speed of the upper PV is faster than that of the w' pattern. Far downwind, the speed of w' is faster and equal to that of the upper PV. The possible explanation is that near the heating source, the effect of IGW is strong, but it decays very fast away from the source. So in the far field, only the effect of the upper drifting PV-pulse is dominant and could trigger perturbations in the lower layer.

In the sections below, we use observed surface pressure to determine the properties of diurnal disturbances.

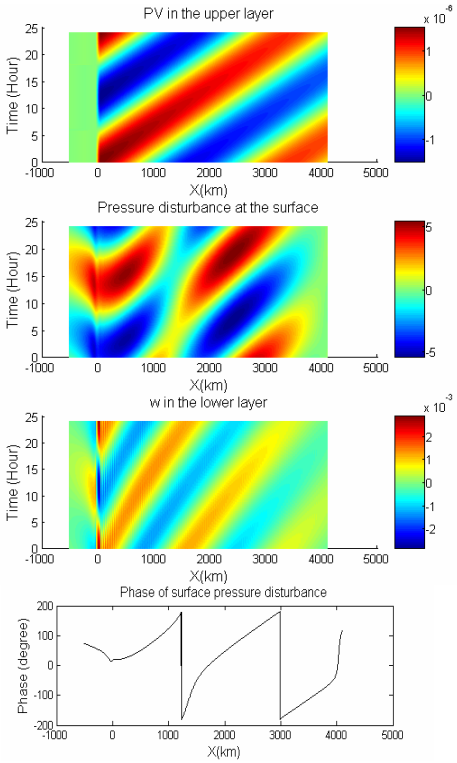

Figure 4: Simulation 3. Strong westerly wind shear, weak Coriolis effect with $f = 10^{-5}s^{-1}$, $U_1/U_2 = 5/40\,m\cdot s^{-1}$. *The time-distance plot of upper PV, surface pressure disturbance and the lower vertical velocity perturbation, and the phase distribution of surface pressure disturbance* $\varphi(x)$.

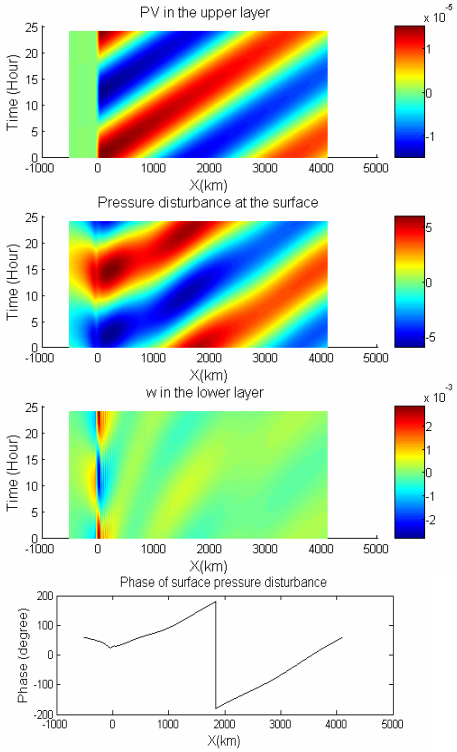

Figure 5: *Simulation 4. Like figure 4 but with strong Coriolis effect* $f = 10^{-4}s^{-1}$.

4. The study of the observed diurnal pressure signals:

4.1 Florida:

Florida is a region with strong land-sea contrast in local diurnal heating. The diurnal component is calculated by averaging summer seasons (JJA) of year 2001, 2002, 2003, 2004. The calculated phase is adjusted to the local solar time. The diurnal pressure signature is weak here, so the mesoscale part is difficult to determine. Here, we take the atmospheric tide in the literature as a reference: $A = 20\,Pascal$, $\theta = 103^{o}$ (Braswell and Lindzen, 1998). After subtracting the estimated atmospheric tide, we get a fairly smooth pattern.

Figure 6 gives the amplitude and phase distributions of the diurnal component of the sea level pressure variations and its mesoscale part. It shows that the amplitude of mesoscale part is around 10 to 20 Pascal. Centers for the phase and the amplitude are displaced from each other. Our linear theory analysis (Figure 3) shows that such a displacement can occur when a mean wind is present.

Considering the low latitude of Florida ($27^{o}N$) and the dominant phenomenon there is sea breeze, it is possible that the pressure perturbations generated by local land heating spread through the whole peninsula by IGW.

Figure 6: The diurnal component (black) and the mesoscale part (amplitude: red, phase: green) of the sea level pressure variations for stations in Florida. Amplitude is in unit Pascal. The red contours show the center of the amplitude. Phase angle is in unit Degree and in local solar time. The green contours show the center of the phase. The atmospheric tide in literature is taken as a reference.

4.2 Great Plains and the Mid-west:

This region (between $38^{o}N$ and $42^{o}N$, $105^{o}W$ and $85^{o}W$) shows a strong diurnal pressure signature. The phases everywhere (relative to Local Solar Time) are quite similar indicating a tide-like behavior (Figure 7, 8). When the average tide vector is subtracted from the data, the residual shows a wide variation in phase (Figure 7, 8). This might be noise, but when the residual phase is plotted against longitude, the scatter reduces and there is a clear slope indicating eastward movement (Figure 9). The speed is about 25m/s. This is probably Carbone's eastward propagating storms. But we still don't know the mechanism: PV pulses, IGW, or storm propagation with cold pool dynamics.

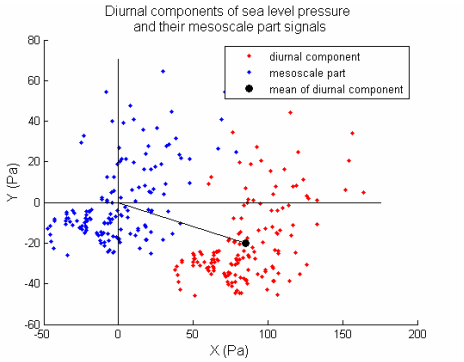

Figure 7: The diurnal component vectors and their mesoscale parts for stations in Great Plains and the Mid-west. The distance between the point and the origin is the amplitude. The angle between the North and the vector is the phase.

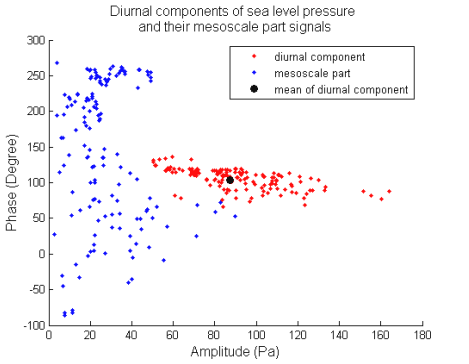

Figure 8: The diurnal component of the sea level pressure variations and the mesoscale part after subtracting the atmospheric tide.

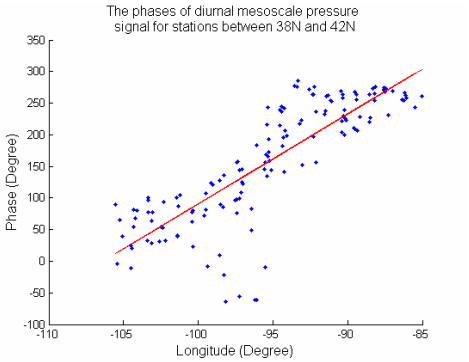

Figure 9: The phase (adjusted to CST) of the mesoscale part vs. longitude. The red line is the result of linear regression.

However, the amplitude of the atmospheric tide we subtracted is about 83 Pascals, 4 times as big as the global

tide. We suppose that this is a "continentally enhanced tide" and is driven by surface heat fluxes, distributed upwards through dry and moist convection.

4.3 Western valleys:

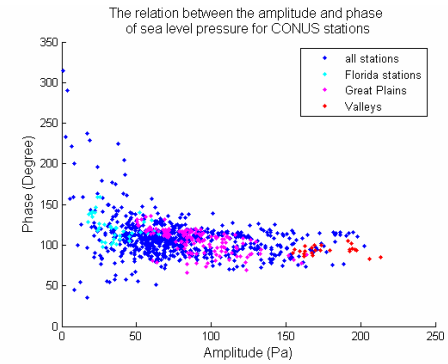

Figure 10: The distributions of the amplitude and the phase of the sea level pressure variations for CONUS stations.

Here, we plot the amplitude and the phase of the sea level pressure variations from nine hundred CONUS stations in Figure 10. It shows an interesting pattern. The stations in dry western valleys have large amplitude, more than 150 Pascal, and relatively early phase, around 90^{o}(Surface pressure reaches its minimum around 1800 in local solar time). Examples include Bishop, Ontario and Rifle (the largest amplitude). This probably represents simple heating of the air trapped in the valleys. No buoyancy adjustment or gravity wave generation can occur because of the valley walls. The tidal correction is almost negligible here as the local signal is so large.

7. Summary and Conclusions:

Table 1: Types of diurnal pressure signals

Region	Amplitude	Phase	Spatial Pattern
Florida	small	Tide + late (1 to 2 hours delay) mesoscale disturbance	Offset phase and amplitude centers
Great Plains and the Mid-West	moderate	Continentally enhanced tide + Eastward moving disturbance	Front Range source, Speed=25m/s
Western Valleys	large	Early (no delay)	Single stations

The studies of the observed diurnal pressure signal in different regions show different properties (Table 1). In Florida, the mesoscale part has a smooth geographic distribution, with offset phase and amplitude centers. The maximum amplitude is about 20Pa. The minimum pressure occurs at the phase center 1900EST ($\psi_n^{'} = 105^{o}$), delayed to 2100EST ($\psi_n^{'} = 135^{o}$) or later at the coast. At Key West, the minimum may not occur until 0200EST ($\psi_n^{'} = 210^{o}$). A typical pattern speed is 15m/s. Here, the observed phase is much greater than the phase predicted by our linear model (ie. 5 hours later).

In Great Plains and the Mid-West, there is a strong atmospheric tide. Its phase is similar to the global tide (about 103^{o}, which is 1852 local solar time for surface pressure to reach its minimum) but its amplitude (83 Pascals) is four time greater. We think it is "continentally enhanced" by surface heat fluxes. Removing the tide reveals an eastward moving disturbance with a speed 25m/s. Its amplitude is about 50Pa over the Great Plains dropping to about 20Pa in the Mid-west. As a coherent pattern, it is present only east of the Rockies. At 105W the pressure minimum for the eastward-moving disturbance occurs at 1200 CST while at 90W the minimum occurs at about 0200 CST the next day. We propose that this is the pressure signature of the propagating precipitation systems described by Carbone et al. (2002).

The largest diurnal pressure signals are found in dry western valleys. The amplitudes exceed 150Pa (=1.5 mb). The phase shows that the minimum pressure occurs at 1800 local solar time, almost 6 hours after local noon when the solar heating reaches its peak. We speculate that this large signal is caused by heating of the air trapped in the valleys. The valley walls prevent any lateral adjustment or gravity wave generation.

8. Acknowledgements:

This research was supported by the National Science Foundation, Division of Atmospheric Sciences (ATM-0112354).

REFERENCES

Banta, R.M. and C.L.B.Schaaf, 1987: Thunderstorm genesis zones in the Colorado Rocky Mountains as determined by traceback of geosynchronous satellite images. *Mon. Wea. Rev.*, **115**, 463-476.

Braswell, W. D. and R. S. Lindzen, 1998: Anomalous short wave absorption and atmospheric tides. *Geophy. Res. Let.*, Vol. 25, No. 9, 1293-1296.

Carbone R.E., J. D. Tuttle, D. A. Ahijvych and S. B. Trier, 2002: Inferences of predictability associated with warm season precipitation episodes. *J. Atmos. Sci.*, **59**, 2033-2056.

Chapman, S., and R. S. Lindzen, 1970: Atmospheric Tides. D. Reidel, 200pp.

Mapes B. E., T. T. Warner and M. Xu, 2003: Diurnal patterns of rainfall in Northwestern South America. Part III: Diurnal gravity waves and nocturnal convection offshore. *Mon. wea. Rev*., **131**, 830-844.

Mass, C. F., W. J. Steenburgh and D. A. Schultz, 1991: Diurnal surface-pressure variations over the continential United states and the influence of sea level reduction. *Mon. Wea. Rev.*, **119**, 2814-2830.

Raymond D. J., H. Jiang, 1990: A theory for long-lived mesoscale convective systems. *J. Atmos. Sci*, **47**, 3067-3077.

Yang G.Y., J. Slingo, 2001: The diurnal cycle in the tropics. *Mon. wea. Rev*., **129**, 784-801.